

Clinically relevant model of oxaliplatin-induced sinusoidal obstruction syndrome

Rei Toda¹  | Satoru Seo¹ | Yusuke Uemoto¹ | Koshiro Morino¹ | Hiroto Nishino¹ | Naohiko Nakamura²  | Masayuki Okuno³ | Kohta Iguchi⁴ | Motohiko Sato¹ | Kojiro Nakamura^{1,5} | Kojiro Taura¹ | Shunsaku Nakagawa⁶ | Takayuki Nakagawa⁶ | Tatsuaki Tsuruyama^{7,8} | Toshiaki Manabe⁹ | Hiroaki Kawaguchi¹⁰ | Keiko Iwaisako^{1,11} | Masaya Ikegawa¹¹ | Shinji Uemoto^{1,12} | Etsuro Hatano¹

¹Department of Surgery, Graduate School of Medicine, Kyoto University, Kyoto, Japan

²Department of Surgery, Kanazawa Medical University, Ishikawa, Japan

³Department of Gastroenterological Surgery, Hyogo Medical University, Nishinomiya, Japan

⁴Department of Gastrointestinal Medicine & Surgery, Tazuke Kofukai Medical Research Institute, Kitano Hospital, Osaka, Japan

⁵Department of Surgery, Kobe City Nishi-Kobe Medical Center, Kobe, Japan

⁶Department of Clinical Pharmacology and Therapeutics, Graduate School of Medicine, Kyoto University, Kyoto, Japan

⁷Department of Drug Discovery Medicine, Division of Pathology, Graduate School of Medicine, Kyoto University, Kyoto, Japan

⁸Department of Diagnostic and Pathology, Graduate School of Medicine, Kyoto University, Kyoto, Japan

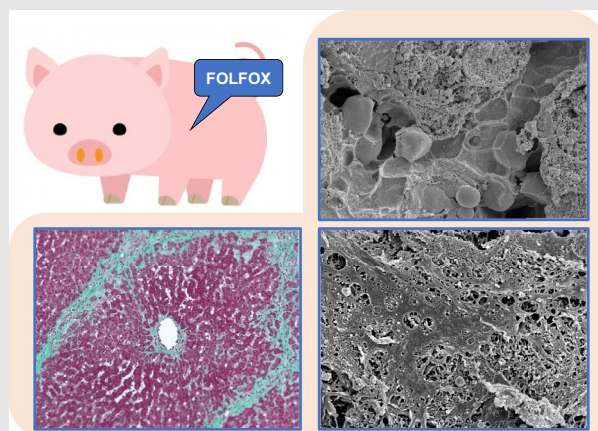
⁹Department of Diagnostic and Pathology, General Incorporated Association PaLaNA Initiative, Otsu, Japan

¹⁰Laboratory of Veterinary Pathology, Kitasato University School of Veterinary Medicine, Aomori, Japan

¹¹Department of Medical Life Systems, Faculty of Life and Medical Sciences, Doshisha University, Kyotanabe, Japan

¹²Shiga University of Medical Science, Otsu, Japan

Graphical Abstract



Sinusoidal obstruction syndrome (SOS) induced by oxaliplatin-including chemotherapies (OXCx) is associated with impaired hepatic reserve and higher morbidity after hepatic resection; however, in the absence of an appropriate animal experimental model, little is known about its pathophysiology. In this study, we established a clinically relevant reproducible model of OXCx-induced SOS and highlighted the disparities and common features between OXCx-SOS and rodent monocrotaline induced SOS. With distinct differences between rodent monocrotaline-SOS and human/pig OXCx-SOS, our pig OXCx-SOS model serves as a preclinical platform for future investigations to dissect the pathophysiology of OXCx-SOS and seek preventive strategies.

Abbreviations: ALT, alanine aminotransferase; Alb, albumin; AST, aspartate aminotransferase; AT-III, antithrombin III; CRLM, colorectal liver metastasis; Hb, hemoglobin; HMGB1, high mobility group box 1; ICG, indocyanine green; I-LV, folinic acid; ISGLS, International Study Group of Liver Surgery; L-OHP, Oxaliplatin; LSEC, liver sinusoidal endothelial cell; MCT, monocrotaline; MMP9, matrix metalloproteinase 9; OS, overall survival; OXCx, Oxaliplatin-including chemotherapies; PHLF, post-hepatectomy liver failure; PLT, platelet; PT, prothrombin time; RECA-1, rat endothelial cell antigen -1; rhTM, recombinant human soluble thrombomodulin; SCT, stem cell transplantation; SEM, scanning electron microscopy; SOS, Sinusoidal obstruction syndrome; T-Bil, total bilirubin; TEM, transmission electron microscopy.

Correspondence

Satoru Seo, Department of Surgery, Graduate School of Medicine, Kyoto University, 54 Kawahara-cho, Shogoin, Sakyo-ku, Kyoto 606-8507, Japan.
Email: rutosa@kuhp.kyoto-u.ac.jp

Funding information

Japan Society for the Promotion of Science, Grant/Award Numbers: 16H05414, 18K08645, 19K24012

Abstract

Aim: Sinusoidal obstruction syndrome (SOS) induced by oxaliplatin-including chemotherapies (OXCx) is associated with impaired hepatic reserve and higher morbidity after hepatic resection. However, in the absence of an appropriate animal experimental model, little is known about its pathophysiology. This study aimed to establish a clinically relevant reproducible model of FOLFOX-induced SOS and to compare the clinical/histopathological features between the clinical and animal SOS settings.

Methods: We performed clinical/pathological analyses of colorectal liver metastasis (CRLM) patients who underwent hepatectomy with/without preoperative treatment of FOLFOX ($n = 22/18$). Male micro-minipigs were treated with 50% of the standard human dosage of the FOLFOX regimen.

Results: In contrast to the monocrotaline-induced SOS model in rats, hepatomegaly, ascites, congestion, and coagulative necrosis of hepatocytes were absent in patients with CRLM with OXCx pretreatment and OXCx-treated micro-minipigs. In parallel to CRLM cases with OXCx pretreatment, OXCx-challenged micro-minipigs exhibited deteriorated indocyanine green clearance, morphological alteration of liver sinusoidal endothelial cells, and upregulated matrix metalloproteinase-9. Using our novel porcine SOS model, we identified the hepatoprotective influence of recombinant human soluble thrombomodulin in OXCx-SOS.

Conclusions: With distinct differences between monocrotaline-induced rat SOS and human/pig OXCx-SOS, our pig OXCx-SOS model serves as a preclinical platform for future investigations to dissect the pathophysiology of OXCx-SOS and seek preventive strategies.

KEYWORDS

colorectal liver metastasis, liver sinusoidal endothelial cell, matrix metalloproteinase 9, micro-minipig, oxaliplatin, sinusoidal obstruction syndrome

INTRODUCTION

In the 1990s, only 25% of patients with colorectal liver metastasis (CRLM) were candidates for curative hepatic resection.¹ Recent advances in systemic chemotherapy have contributed to converting initially unresectable CRLM to resectable lesions, which is a process called conversion therapy.² In 2004, systemic cytotoxic chemotherapy regimens enabled 12.5% of initially unresectable CRLM to undergo hepatic resection, leading to a 5-year overall survival (OS) rate of 33%.³ In our recent prospective clinical study of initially patients with unresectable CRLM, the combination of cytotoxic chemotherapy with molecular targeted agents achieved a 70.6% conversion rate and 50.0% R0 resection rate; ultimately patients with R0/1 liver resection showed a 5-year OS of 66.3%.^{2,4} These results indicate the effectiveness of the combination of chemotherapy and surgery to improve the outcome of patients with CRLM.

Oxaliplatin (L-OHP)-including chemotherapies (OXCx), such as FOLFOX, CAPOX, or FOLFOXIRI, are key regimens for the treatment of CRLM. Patients are treated with intense OXCx before conversion hepatectomy; however, the extensive use of OXCx causes toxicity to

the non-tumorous liver parenchyma. Sinusoidal obstruction syndrome (SOS), a drug-induced hepatic injury triggered by the damage of liver sinusoidal endothelial cells (LSECs), occurs from the administration of myeloablative, high-dose chemotherapy in the setting of stem cell transplantation (SCT-SOS). Rubbia-Brandt *et al.* found that OXCx causes SOS (OXCx-SOS),⁵ which is associated with increased postoperative morbidity^{6,7} and shorter long-term survival.⁸ Hence, preventive strategies against OXCx-SOS and elucidation of the pathophysiology of OXCx-SOS development are needed.

The majority of SCT-SOS cases occur within 21 days from toxic insult, with clinical manifestations of weight gain, hepatomegaly, hyperbilirubinemia, and ascites (modified Seattle or Baltimore criteria).⁹ The most widely used animal model of SOS is generated by administration of monocrotaline (MCT) to rats,^{10,11} which induces a sharp onset of SOS, mimicking symptomatic SCT-SOS. In contrast to SCT-SOS and MCT-SOS, OXCx-SOS develops more gradually and asymptotically, implying that OXCx-SOS may be divergent from SCT-SOS and MCT-SOS. Several previous studies reported that OXCx treatment induced SOS in mice or rats.¹²⁻¹⁴ However, the OXCx-based rodent SOS models have faced limited reproducibility.¹⁵⁻¹⁷ Therefore,

establishing a clinically applicable experimental model of OXCx-SOS is critical to explore its pathophysiology and develop prophylactic strategies.

In this study, we established a clinically relevant model of OXCx-SOS using micro-minipigs. We highlight the differences and similarities between SCT-SOS (human), MCT-SOS (rat), and OXCx-induced human/pig SOS. Using the novel pig OXCx-SOS model, we identified the hepatoprotective role of recombinant human soluble thrombomodulin (rhTM), which is reported to alleviate rodent MCT-SOS.^{18,19} In the context of a first-in-class drug being applied for severe human SCT-SOS,^{20–22} our pig OXCx-SOS model serves as a preclinical platform to dissect the pathophysiology of OXCx-SOS.

METHODS

Patient selection and non-tumorous liver tissue evaluation

We performed clinical and pathological analyses of CRLM cases treated with hepatectomy at Kyoto University Hospital (April 2007–February 2020). Patients treated with preoperative chemotherapy regimen without FOLFOX and patients whose non-tumorous lesion was insufficient for histological evaluations were excluded. The identified 40 patients were divided into the group that received preoperative treatment of FOLFOX (OXCx group, $n = 22$) and the group without any chemotherapy (control group, $n = 18$) before liver resection. Serum aspartate aminotransferase (AST), alanine aminotransferase (ALT), total bilirubin (T-Bil), albumin levels, and prothrombin time were measured as a routine preoperative assessment. The indocyanine green (ICG) clearance test was performed to evaluate liver function just before hepatic resection. Postoperative morbidity was evaluated based on the Clavien–Dindo classification.²³ The International Study Group of Liver Surgery criteria were used to identify post-hepatectomy liver failure.²⁴ Non-tumorous liver tissue was evaluated by hematoxylin and eosin staining, Masson trichrome staining, electron microscopy, and immunohistochemistry. Based on preoperative computed tomography examinations, splenic coefficients were calculated by multiplying maximal length (cm) by vertical height (cm), and then patients with the values over the cut-off of 115 cm² were diagnosed as splenomegaly.²⁵ The study was approved by the Ethics Committee of Kyoto University Graduate School and Faculty of Medicine (approval code: R3004).

Animals

Male Sprague–Dawley rats (8–9 weeks old, 300 ± 50 g) and male C57BL/6 mice (8–10 weeks, 25 ± 5 g) were obtained from SLC. Male-specific pathogen-free micro-minipigs (1–1.5 years old, 25 kg) were obtained from Fuji Micra. All experiments were approved by the Animal Research Committee of Kyoto University (Med Kyo 18187). The animals received humane care and the protocols

complied with institutional guidelines for the care and use of laboratory animals.

Reagents

MCT was purchased from Sigma-Aldrich and used as a 10 mg/ml solution.^{11,26} L-OHP was provided by Yakult Honsha and rhTM was a gift from Asahi Kasei Pharma. Folinic acid (I-LV), fluorouracil (5-FU), and ICG were obtained from Daiichi Sankyo.

Monocrotaline-induced sinusoidal obstruction syndrome rat model

Rats were fasted for 12 h before oral administration of MCT (90 mg/kg) with free access to water; subsequently animals were allowed food and water ad libitum.^{18,27,28} Blood and liver samples were collected at various time points after MCT administration. To investigate the impact of MCT-SOS on the mortality of animals undergoing minimal liver resection, a 30% partial hepatectomy was performed in the other rats. The animals were monitored for 10 days and those who were alive at this time point were considered survivors.

FOLFOX administration model in mice

Based on the previous studies,^{12,13} C57BL/6 mice were treated with an intraperitoneal injection of L-OHP 6 mg/kg, followed by 5-FU 50 mg/kg and I-LV 90 mg/kg 2 h later on a weekly basis for 5 weeks. Control animals received vehicle alone. Mice were fed on a standard purified diet (D01060501; Research Diets Inc.) instead of a standard chow diet.^{12,13} All animals received standard animal house care, including ad libitum access to water and the purified diet. Mice were killed 1 week after the final dose of chemotherapy, and blood and liver samples were obtained. Serum AST and ALT levels were evaluated in serum samples. Liver samples were evaluated by light microscopy and electron microscopy.

OXCx-induced sinusoidal obstruction syndrome model in micro-minipigs

To mimic the clinical mFOLFOX6 protocol and accurately inject chemotherapeutic agents in micro-minipigs, we first placed a central venous access port (BD, San Jose, CA, USA) in a femoral vein under inhalational anesthesia (isoflurane, 0.5%–3%). Before the procedure, pigs were sedated with midazolam (0.4 mg/kg), medetomidine (0.08 mg/kg), and atropine sulfate (0.02 mg/kg) intramuscularly and with buprenorphine hydrochloride (0.08 mg/kg) for analgesia. Based on preliminary experiments, we selected the optimal dosage of FOLFOX regimen as L-OHP 42.5 mg/m², I-LV 100 mg/m², bolus 5-FU

200 mg/m², and continuous 5-FU 1200 mg/m², which was 50% of the standard human dosage (L-OHP, 85 mg/m²; I-LV, 200 mg/m²; bolus 5-FU, 400 mg/m²; and continuous 5-FU, 2400 mg/m²). Pigs in the OXCx group (*n* = 5) were treated with this regimen every other week, while pigs in the control group (*n* = 5) were administered with vehicle every other week. Pigs were treated with OXCx or vehicle for up to 12 cycles. Liver/blood samples were obtained at 2 weeks after the beginning of the 12th cycle or earlier time points (2 weeks after the beginning of a cycle, before the start of the next regimen if scheduled). Animals were given supportive care such as antiemetics (palonosetron hydrochloride, 0.75 mg) for nausea/vomiting or transfusion of lactated Ringer's solution for symptoms of dehydration whenever necessary. Hepatic histopathological assessments were performed in a blinded fashion by pathologists (Tatsuaki Tsuruyama and Toshiaki Manabe). Livers in the OXCx group exhibited histopathological SOS features after 9–12 cycles of regimen. Serum AST, ALT, T-Bil, blood hemoglobin levels, platelet count, and antithrombin III activity were measured. The ICG test was also performed to assess liver function. ICG (0.5 mg/kg) was administered intravenously, and the ICG-K value was measured to determine its rate of clearance from the serum.²⁹ To evaluate the hepatoprotective influence of rhTM (500 µg/kg) in the porcine OXCx-SOS model, rhTM was injected intravenously at 30 min before the beginning of each cycle.

Serum platinum concentration evaluation

We measured serum platinum concentrations at the end of each L-OHP infusion using an Agilent 7700 inductively coupled plasma-mass spectrometer (Agilent Technologies).

Statistical analysis

For animal experiments, comparisons between two groups were assessed using a two-tailed Student's *t*-test. For human data, continuous values were analyzed by Mann–Whitney *U*-test and categorical variables by Fisher's exact test. Survival curves were generated using the Kaplan–Meier method and were compared using a log-rank test. *p* < 0.05 was considered statistically significant. JMP for Windows 14.0 (SAS Institute, Cary, NC, USA) was used for all the statistical analyses.

Please see Supporting Information S1 for additional methods.

RESULTS

OXCx leads to deterioration in liver function without hepatomegaly, ascites, hyperbilirubinemia, or elevation of hepatic transaminases in patients with colorectal liver metastasis

To assess the influence of preoperative OXCx on clinical features, liver function, and histological changes in patients with CRLM, we

compared patients who underwent primary hepatectomy at Kyoto University Hospital with preoperative treatment of FOLFOX (OXCx group, *n* = 22) and those who did not receive chemotherapy (control group, *n* = 18) before liver resection. Perioperative variables of the patients are listed in Table 1. Age, sex, colorectal cancer status, comorbidity, and preoperative hepatic tests were comparable between the two groups. In the OXCx group, synchronous (72.7% vs. 27.8%) and multiple (100% vs. 44.4%) CRLM were more frequent. Of the 22 patients, 18 (81.8%) were treated with six or more OXCx cycles before hepatectomy. In the OXCx group, eight patients were treated with bevacizumab (median cycles of seven), six with cetuximab (median cycles of six), and four with panitumumab (median cycles of eight). The median interval between the last chemotherapy and hepatic resection was 57.5 days (range, 20–392 days). Major hepatectomy was performed in 40.9% and 50.0% of patients in the OXCx and control group, respectively, while laparoscopic surgery was conducted in 13.6% and 27.8%, respectively. Morbidity (≥Clavien–Dindo classification I)²³ and post-hepatectomy liver failure²⁴ tended to be more frequent in the OXCx group; however, the differences were not statistically significant.

None of the patients in the OXCx group were diagnosed as splenomegaly preoperatively, with the median of splenic coefficient of 66.3 (range, 26.9–105.1). Notably, OXCx did not induce hepatomegaly, peritoneal fluid collection, or elevated serum bilirubin levels (Table 1), which are typical clinical characteristics of SCT-SOS.⁹ Preoperative OXCx was associated with decreased ICG-K values (*p* < 0.05) compared with the value in the control group (Figure 1a), indicating OXCx was associated with a deterioration in liver function. Comparison of AST/ALT levels before OXCx and after chemotherapy (just before surgery) revealed that OXCx had no effect on serum transaminase levels (Table 1). Macroscopically, the liver surface in the OXCx group showed a patchy pattern (Figure 1b). In the OXCx group, hematoxylin and eosin and Masson trichrome staining of the non-tumorous area showed sinusoidal dilatation, and collagen deposition to the perisinusoidal space and around the central vein; however, sinusoidal congestion, occlusion of the central vein, and coagulative necrosis of hepatocytes, which are typical histological appearances in human SCT-SOS and rat MCT-SOS, were not observed (Figure 1c,d).

Preoperative OXCx is associated with morphological alteration of liver sinusoidal endothelial cells, disruption of liver sinusoidal endothelial cell integrity and matrix metalloproteinase-9 increase in non-tumorous livers in patients undergoing hepatectomy

Initial morphological changes of LSECs (a dish-like transformation), following matrix metalloproteinase (MMP)-9 upregulation, enlargement of the space of Disse, and discontinuity of sinusoidal endothelium are key pathophysiology phenomena reported in the rat MCT-SOS model.^{26,27} Whether these events occur during the pathogenesis of human OXCx-SOS remains unknown. We next

TABLE 1 Clinical variables of patients who underwent primary hepatectomy with preoperative treatment of FOLFOX (OXCx group) or without chemotherapy (control group) before surgery and immunohistochemical evaluation of LSECtin

	Control (n = 18)	OXCx (n = 22)	p value	
Age (years)	68 (52–81)	60 (35–80)	0.053	
Sex (male)	11 (61.1%)	15 (68.2%)	0.64	
Colorectal tumor				
Rectum/colon	4/13	5/16	0.97	
Sidedness (right)	5 (27.8%)	5 (22.7%)	0.73	
T factor (T1/T2/T3/T4)	0/2/12/6	2/0/10/5	0.26	
Positive lymph metastases	11 (61.1%)	10/16 (62.5%)	0.93	
Extrahepatic metastases	2 (11.1%)	4 (18.2%)	0.53	
Liver lesion				
Synchronous	5 (27.8%)	16 (72.7%)	<0.01	
Maximum diameter (cm)	8.2 (0.3–90)	3.0 (0.3–90.0)	0.24	
Multiple	8 (44.4%)	22 (100%)	<0.01	
Hepatic vein invasion	1 (5.6%)	1 (4.6%)	0.88	
Portal vein invasion	1 (5.6%)	0 (0%)	0.26	
Surgical margin (positive)	1 (5.6%)	1 (4.6%)	0.88	
Comorbidity				
Diabetes	2 (11.1%)	2 (9.1%)	0.66	
Hepatitis virus (HBV/HCV)	0/0	1/0	0.99	
Preoperative chemotherapy				
Yes	0 (0%)	22 (100%)	-	
≥6 FOLFOX	-	18 (81.8%)	-	
With bevacizumab	-	8 (36%)	-	
With cetuximab	-	11 (50%)	-	
With panitumumab	-	4 (18%)	-	
Preoperative hepatic test				
AST (IU/L)	25 ± 7	34 ± 18	0.08 ^a	0.15 ^b
ALT (IU/L)	23 ± 10	28 ± 25	0.98 ^a	0.81 ^b
T-Bil (mg/dl)	0.7 ± 0.2	0.8 ± 0.4	0.27 ^a	0.37 ^b
Alb (g/dl)	4.0 ± 0.4	3.8 ± 0.5	0.42 ^a	0.94 ^b
PT (%)	100 ± 13	100 ± 26	0.43 ^a	0.44 ^b
Hepatic test before FOLFOX				
AST (IU/L)	-	28 ± 15	-	
ALT (IU/L)	-	26 ± 20	-	
T-Bil (mg/dl)	-	0.7 ± 0.3	-	
Alb (g/dl)	-	3.8 ± 0.6	-	
PT (%)	-	97 ± 18	-	
Liver surgery				
Major hepatectomy	9 (50.0%)	9 (40.9%)	0.57	
Laparoscopic hepatectomy	5 (27.8%)	3 (13.6%)	0.27	
Morbidity (>CD-I)	3 (16.7%)	7 (31.8%)	0.72	
PHLF	0 (0%)	1 (4.6%)	0.99	

(Continues)

TABLE 1 (Continued)

	Control (n = 18)	OXCx (n = 22)	p value
Operative finding			
Hepatomegaly	0 (0%)	0 (0%)	-
Ascites	0 (0%)	0 (0%)	-
Histological finding			
LSEctin positive area (%)	2.9 ± 0.5	1.0 ± 0.8	<0.01

Note: Bold values signifies p values less than 0.05.

Abbreviations: Alb, albumin; ALT, alanine aminotransferase; AST, aspartate aminotransferase; CD-I, Clavien–Dindo classification grade I; HBV, hepatitis B virus; HCV, hepatitis C virus; LSEctin, liver sinusoidal endothelial cell lectin; OXCx, oxaliplatin including chemotherapy; PHLF, post-hepatectomy liver failure. PT, platelets; T-Bil, total bilirubin.

^aComparison of preoperative hepatic test results of control versus OXCx groups.

^bComparison of hepatic test results in OXCx group before versus after OXCx administration.

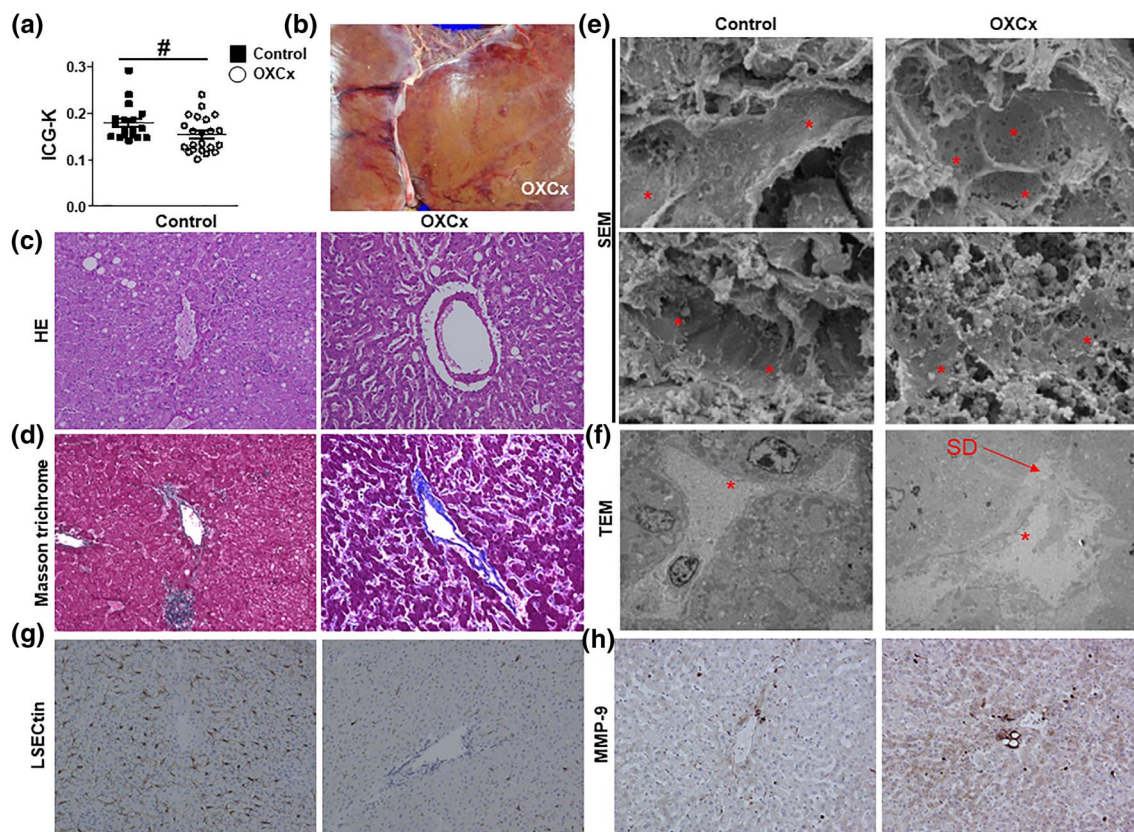


FIGURE 1 Oxaliplatin-including chemotherapy (OXCx) before hepatectomy for patients with colorectal liver metastasis (CRLM) is associated with sinusoidal dilatation, collagen deposition, damage on liver sinusoidal endothelial cells (LSECs), increased matrix metalloproteinase-9 (MMP-9) expression, and deterioration in liver function. Forty patients who underwent primary hepatectomy with preoperative treatment of OXCx (OXCx group, $n = 22$) or without chemotherapy (control group, $n = 18$) before surgery were compared. (a) Indocyanine green elimination rate (ICG-K) in the control and OXCx groups ($\#p < 0.05$). Data are shown as mean \pm standard error of the mean. (b) Representative macroscopic view of resected liver specimens (left hemi-hepatectomy) in the OXCx group. (c) Representative hematoxylin and eosin stains ($\times 200$). (d) Representative Masson trichrome stains ($\times 200$). (e) Representative scanning electron microscopy (SEM) images (original magnification, top; $\times 4000/\times 4000$, bottom; $\times 4000/\times 4000$). (f) Representative transmission electron microscopy (TEM) images (original magnification, $\times 1000/\times 1000$). *LSEC; SD, space of Disse. (g) Representative images of immunohistochemical staining for LSEC lectin (LSEctin; $\times 200$). (h) Representative images of immunohistochemical staining for MMP-9 ($\times 200$)

evaluated whether OXCx induces these phenomena in human liver. Scanning electron microscopic evaluation revealed dish-like morphological changes of LSECs and disruption of LSEC integrity in the OXCx group in contrast to the control liver (Figure 1e). Transmission electron microscopic examination showed disruption of LSEC lining, uplift of LSEC, and enlargement of the space of Disse (Figure 1f). To examine the retention of LSECs, we conducted immunohistochemical staining for LSEC lectin. In the OXCx group, LSEC lectin-expressing areas were significantly decreased compared with expression in the control group (Figure 1g and Table 1, $p < 0.01$). Liver sections in the OXCx group showed enhanced MMP-9 expression compared with expression in control livers. These findings indicate that OXCx-induced hepatic injury was accompanied by LSEC damage and MMP-9 upregulation.

Monocrotaline causes acute sinusoidal obstruction syndrome in rat with hepatomegaly, bloody ascites, coagulative hepatocellular necrosis, abundantly elevated serum transaminase levels and lethality when undergoing 30% of liver resection

Having identified the characteristics of human OXCx-SOS (Table 1, Figure 1), we compared the observations in the commonly used rat MCT-SOS model^{11,26} with human OXCx-SOS. In contrast to the observations in human OXCx-SOS, MCT treatment in rats led to hepatomegaly, bloody peritoneal fluid (Figure 2a), congestion, and coagulative necrosis of hepatocytes (Figure 2b), all of which represent SCT-SOS. Hepatic injury developed as early as 48 h after MCT gavage (Figure 2a,b), with highly elevated transaminase levels (Figure 2c). MCT-treated mice exhibited deteriorated

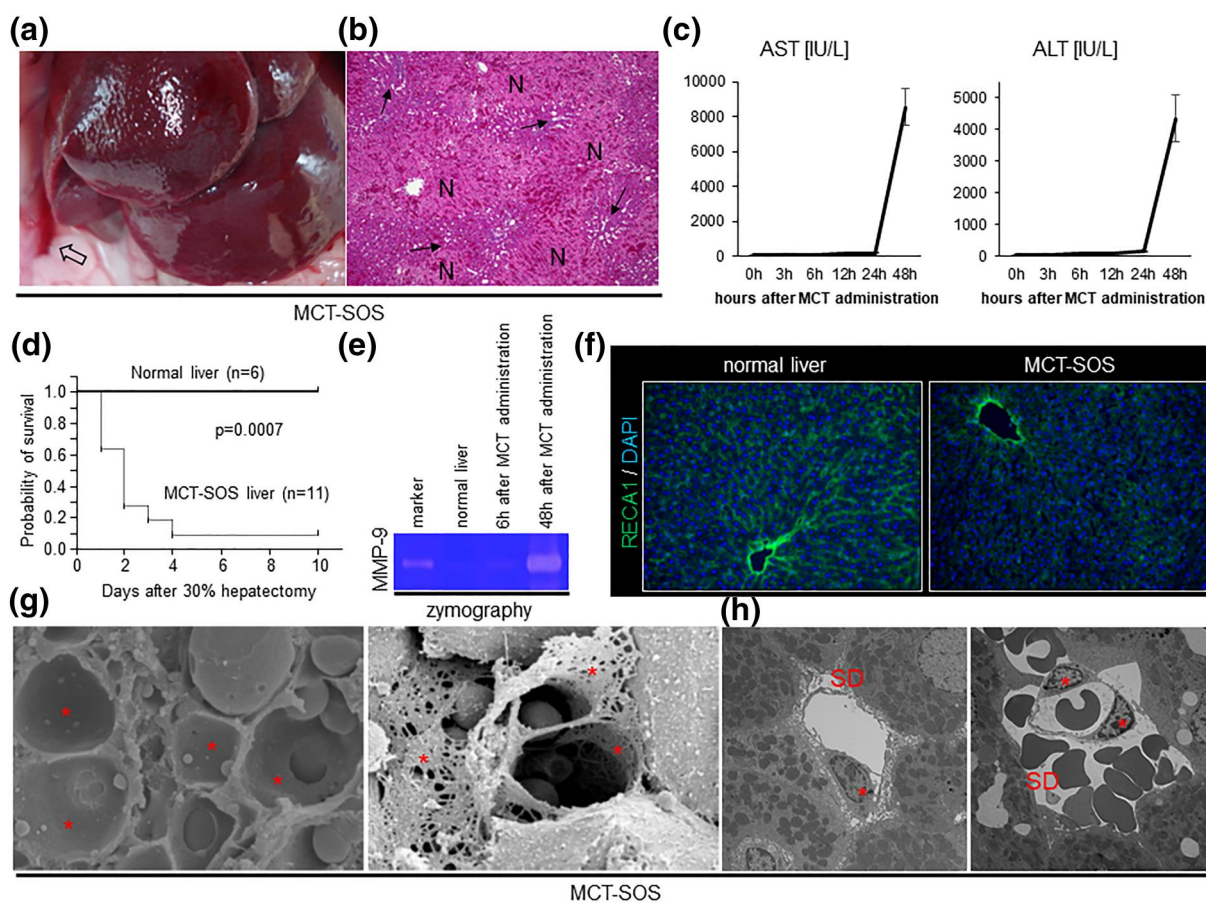


FIGURE 2 Monocrotaline (MCT) causes acute progressing sinusoidal obstruction syndrome (SOS) in rats with liver sinusoidal endothelial cell (LSEC) injury and augmented matrix metalloproteinase (MMP)-9 enzymatic activity, leading to decreased survival after hepatectomy. (a) Representative macroscopic view of rat liver at 48 h after MCT administration. Blank arrow indicates bloody ascites. (b) Representative hematoxylin and eosin images of rat livers at 48 h after MCT administration ($\times 100$). Arrows: sinusoidal dilatation. N, necrotic area. (c) Serum aspartate aminotransferase (AST; left panel) and alanine aminotransferase (ALT; right panel) levels at 0, 3, 6, 12, 24, and 48 h after MCT administration ($n = 5-9$ /each). Data are shown as mean \pm standard error of the mean. (d) Kaplan-Meier curves for 10-day survival after 30% partial hepatectomy in naive rats and rats gavaged with MCT at 48 h before surgery. (e) Enzymatic activity of MMP-9 in naive and MCT-injured liver was evaluated by gelatin zymography. (f) Representative immunohistochemical images of rat endothelial cell antigen-1 (RECA-1) ($\times 200$). DAP, 4',6-diamidino-2-phenylindole. (g) Representative scanning electron microscopic images (original magnification, left panel, $\times 8000$; right panel, $\times 3000$). (h) Representative transmission electron microscopic images (original magnification, left panel, $\times 2000$; right panel, $\times 1500$). *LSEC; SD, space of Disse

postoperative survival when undergoing 30% partial hepatic resection, which was safely performed in naïve mice (Figure 2d). These data indicate that the rat MCT-SOS model mimics human SCT-SOS, while human OXCx-SOS is distinct from rat MCT-SOS in some respects (Table 2).

Monocrotaline upregulates hepatic matrix metalloproteinase-9 in rats, simultaneously influencing the morphology and continuity of liver sinusoidal endothelial cells

Similar to observations in human OXCx-SOS, MCT-SOS livers had augmented MMP-9 enzymatic activity as evidenced by gelatin zymography (Figure 2e). In addition, MCT-SOS livers showed sinusoidal dilatation (Figure 2b), with immunohistochemical staining for rat endothelial cell antigen-1 showing decreased LSECs in MCT-treated rats (Figure 2f). Scanning electron microscopy images exhibited dish-like rounding up of LSECs and damaged LSECs (Figure 2g). Transmission electron microscopy images showed deteriorated LSEC lining and uplift of LSEC, with the spaces of Disse enlarged and filled with red blood cells (Figure 2h). These results indicate that MCT-SOS shares several common pathophysiology phenomena with human

OXCx-SOS including MMP-9 upregulation and LSEC injury, despite several differences (Table 2).

FOLFOX administration fails to induce sinusoidal obstruction syndrome in mice

We next attempted to generate FOLFOX-induced SOS in mice. Following the reported experimental protocol, mice fed on a specific purified diet (D01060501) were treated with or without the FOLFOX regimen^{12,13} (Supporting Information S1: Figure S1a). Of 12 mice in the FOLFOX group, seven mice died before the end of the experimental period, while all mice in the control group survived. FOLFOX administration did not increase serum AST or ALT levels (Supporting Information S1: Figure S1b), and FOLFOX-treated mouse livers did not show sinusoidal dilatation, congestion, and coagulative necrosis (Supporting Information S1: Figure S1c). Immunohistochemistry for CD31 showed preserved LSECs in FOLFOX-injected murine livers (Supporting Information S1: Figure S1d). Electron microscopic examinations revealed a well-preserved LSEC lining on the sinusoidal lumen, without LSEC changes or enlargement of the spaces of Disse. These results indicate that FOLFOX treatment in mice did not cause LSEC injury or hepatocellular death.

TABLE 2 Clinicopathological features of clinical SOS and SOS animal models

Time course	Human SCT-SOS Acute	Rat MCT-SOS Acute	Human OXCx-SOS Chronic	Pig OXCx-SOS Chronic
Clinical findings				
Hepatomegaly	+	+	–	–
Ascites	+	+	–	–
Hyperbilirubinemia	+	+	–	–
Elevation of liver transaminases	+	+	–	–
Deteriorated ICG clearance	Unknown	Unknown	+	+
Histological findings				
Coagulative necrosis	+	+	Minimal	Minimal
Sinusoidal congestion	+	+	Minimal	Minimal
Occlusion of central vein	+	+	Minimal	Minimal
Sinusoidal dilatation	+	+	+	+
Enlargement of the space of Disse	+	+	+	+
Perisinusoidal fibrosis	+	+	+	+
Fibrosis around the central vein	+	+	+	+
Pathophysiology				
Rounding-up of LSEC	+	+	+	+
Loss of endothelial integrity	+	+	+	+
MMP-9 upregulation	+	+	+	+

Abbreviations: ICG, indocyanine green; LSEC, liver sinusoidal endothelial cell; MCT, monocrotaline; MMP-9, matrix metalloproteinase-9; OXCx, oxaliplatin-including chemotherapy; SCT, stem cell transplantation; SOS, sinusoidal obstruction syndrome.

FOLFOX-induced sinusoidal obstruction syndrome model in the micro-minipig

Having failed to develop SOS using FOLFOX in mice, which was consistent with studies unsuccessful in generating FOLFOX-induced SOS in mice or rats,^{15,16} we next aimed to create an OXCx-SOS model using the micro-minipig. Mimicking the clinical mFOLFOX6 method, a central venous access port was placed for each pig in a femoral vein under general anesthesia to robustly infuse anticancer agents (Figure 3a). Infusion pump filled with vehicle (control group) or chemotherapeutic agents (OXCx group) was located at the backside of pigs during the 48 h of infusion (Figure 3b). In preliminary experiments using 100% (L-OHP, 85 mg/m²; I-LV, 200 mg/m²; bolus 5-FU, 400 mg/m²; and continuous 5-FU, 2400 mg/m²) or 75% (L-OHP, 63.75 mg/m²; I-LV, 150 mg/m²; bolus 5-FU, 300 mg/m²; and continuous 5-FU, 1800 mg/m²) of human mFOLFOX6 regimen, all the pigs died at the early time period of the experimental protocol (Supporting Information S1: Table S1). After adjusting to 50% of the human mFOLFOX6 dosage (L-OHP, 42.5 mg/m²; I-LV, 100 mg/m²; bolus 5-FU, 200 mg/m²; and continuous 5-FU, 1200 mg/m²) in a cycle (Figure 3c) and repeating

this regimen every other week, all animals survived (Supporting Information S1: Table S1). Representative pathological SOS characteristics appeared after 9–12 cycles of FOLFOX administration, which is equivalent to 4.5–6 cycles of human mFOLFOX6 (Figure 3d). To estimate the chemotherapeutic intensity in the pig OXCx-SOS model, the peak platinum concentrations were measured (Fig. 3c,e). Consistent with L-OHP administration at 50% of the human dose, the peak blood concentration of platinum after each administration was approximately 50% of the optimal blood concentration in humans.^{30,31}

OXCx induces sinusoidal dilatation, fibrosis, matrix metalloproteinase-9 upregulation, liver sinusoidal endothelial cell injury, enlarged space of Disse, and deterioration in liver function in pigs

Consistent with observations in human OXCx-SOS, pigs treated with FOLFOX showed no hepatomegaly or ascites (Table 2). The liver surface turned slightly patchy and pale after 12 cycles of FOLFOX (Figure 4a), whereas no apparent splenomegaly was observed in

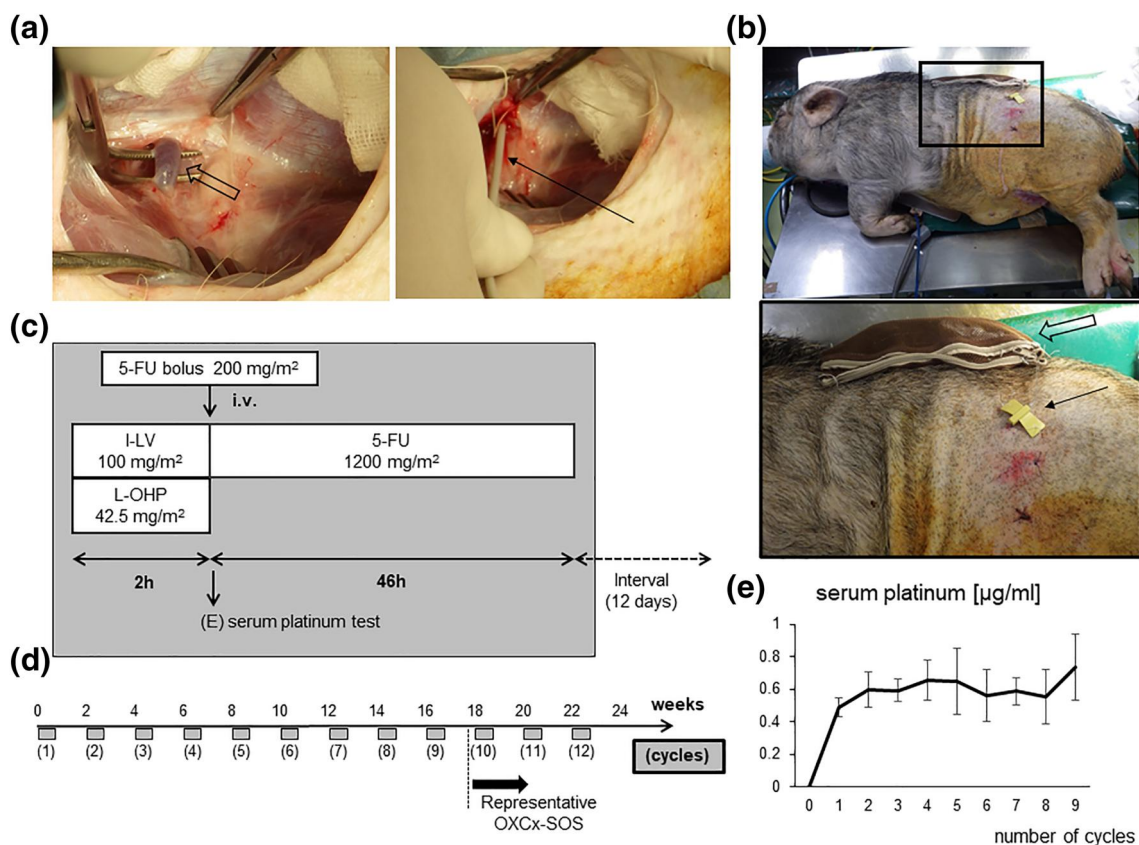


FIGURE 3 Experimental protocol of OXCx-induced sinusoidal obstruction syndrome (SOS) model in pigs. (a) Intraoperative images of placement of a central venous access port. Open arrow indicates a femoral vein. Filled arrow indicates a catheter sheath inserted into a femoral vein. (b) A central venous access port was located at hypodermic space on the backside of animals. Blank arrow indicates an infusion pump filled with normal saline (control group) or anticancer agent (OXCx group). Filled arrow indicates a Huber-point needle. (c) Experimental chemotherapy regimen in a cycle. I-LV, leucovorin; L-OHP, oxaliplatin; 5-FU, fluorouracil. (d) Established OXCx-induced SOS model. (e) Serum samples were collected just after the termination of L-OHP (oxaliplatin) infusion in each cycle, and serum platinum concentration was measured. Data are shown as mean \pm standard error of the mean

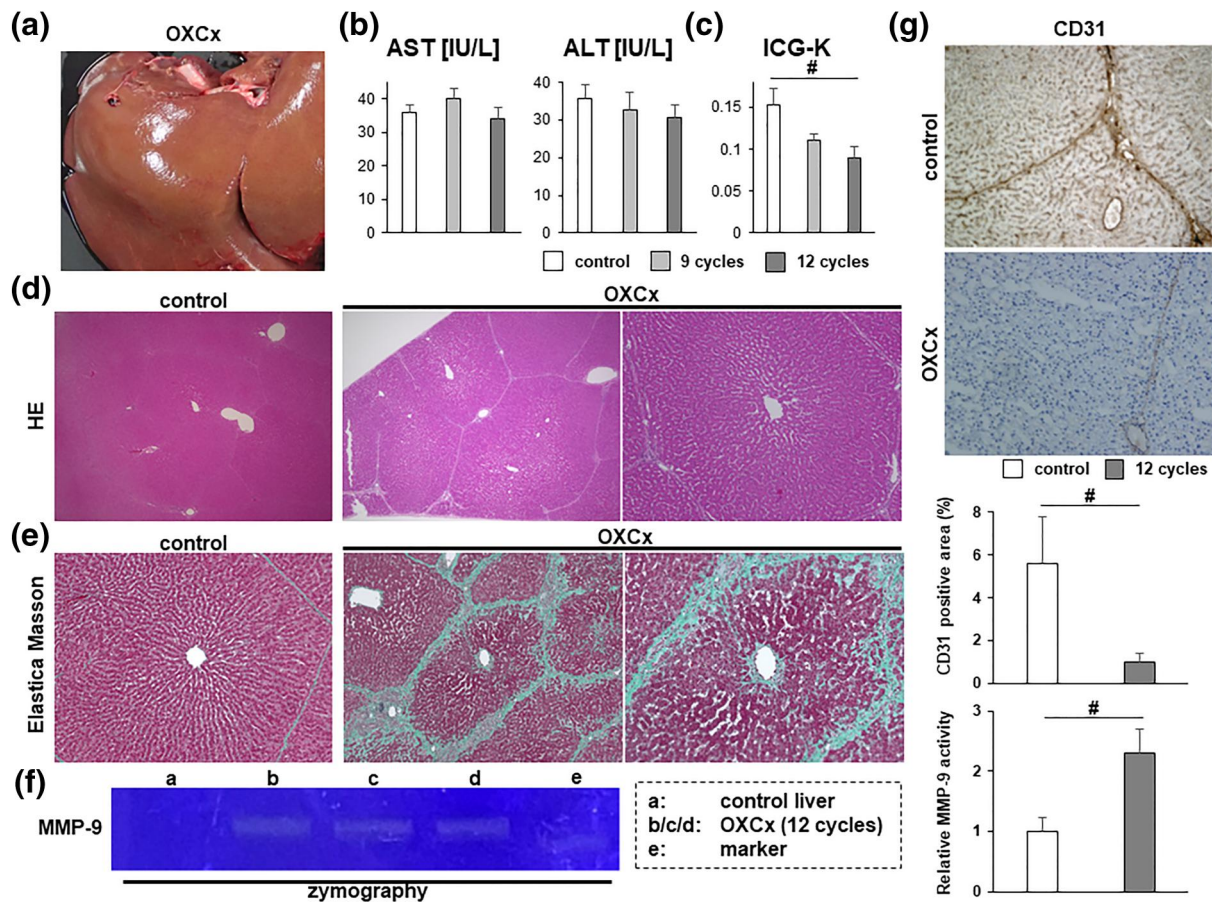


FIGURE 4 OXCx causes deterioration of indocyanine green (ICG) clearance, sinusoidal dilatation, collagen deposition, augmentation of matrix metalloproteinase (MMP)-9, and loss of liver sinusoidal endothelial cell (LSEC) in pigs. (a) Representative macroscopic views of OXCx-treated pig liver. (b) Serum aspartate aminotransferase (AST) and alanine aminotransferase (ALT) levels in the control or OXCx-treated animals. (c) ICG elimination rate (ICG-K) in the control and OXCx-administered livers. (d) Representative hematoxylin and eosin (HE) stains (left/middle panel, $\times 40$; right panel, $\times 100$). (e) Representative Elastica–Masson stains (left/middle panel, $\times 40$; right panel, $\times 100$). (f) A representative zymographic image of MMP-9 activity in control or OXCx-treated livers (left panel) and quantification of relative MMP-9 enzymatic activity by measuring the diminished absorbance of Coomassie blue-stained gelatin gels (right panel). (g) Representative images of immunohistochemical staining for CD31 ($\times 200$) (upper panels) and quantification of CD31-positive area (lower panel). Data are shown as mean \pm standard error of the mean. # $p < 0.05$

FOLFOX-challenged pigs. In contrast to rat MCT-SOS, FOLFOX administration in pigs did not influence serum AST/ALT levels (Figure 4b); hemoglobin level, platelet count, T-Bil level, and antithrombin-III activity were unchanged throughout the experimental period (Supporting Information S1: Figure S2). In parallel to suppressed ICG clearance in the clinical OXCx group (Figure 1a), the ICG-K values in the porcine OXCx group decreased after 12 cycles of the FOLFOX regimen compared with the control pigs (Figure 4c, $p < 0.05$). In accordance with human OXCx-SOS, porcine livers in the OXCx group showed dilatation of sinusoid, whereas sinusoidal congestion, occlusion of central vein and coagulative necrosis of hepatocytes was quite limited (Figure 4d). Elastica–Masson staining showed collagen deposition at perisinusoidal space and around the central vein in the OXCx group (Figure 4e). MMP-9 activity in pigs was augmented after 12 cycles of FOLFOX (Figure 4f, $p < 0.05$). Immunohistochemical detection of endothelial cells (CD31) showed decreased LSECs in the OXCx-treated livers (Figure 4g, $p < 0.05$).

Compared with results in the control liver (Figure 5a), scanning electron microscopy evaluation of FOLFOX-treated pig livers showed dish-like transformation of LSECs (Figure 5b,c), enlarged fenestra of LSECs and damaged LSECs with discontinuous sinusoidal lining (Figure 5d–f). In contrast to results in the control group (Figure 5g), transmission electron microscopic examination revealed lack of LSEC lining (Figure 5h), enlargement of the space of Disse (Figure 5h–j) and collagen fiber in the space of Disse (Figure 5j). Hence, we established a porcine OXCx-SOS model that mimics human OXCx-SOS (Table 2).

Recombinant human soluble thrombomodulin attenuates porcine OXCx-sinusoidal obstruction syndrome

Using the established pig OXCx-SOS model, we next examined whether rhTM decreased SOS severity in OXCx-SOS. In the

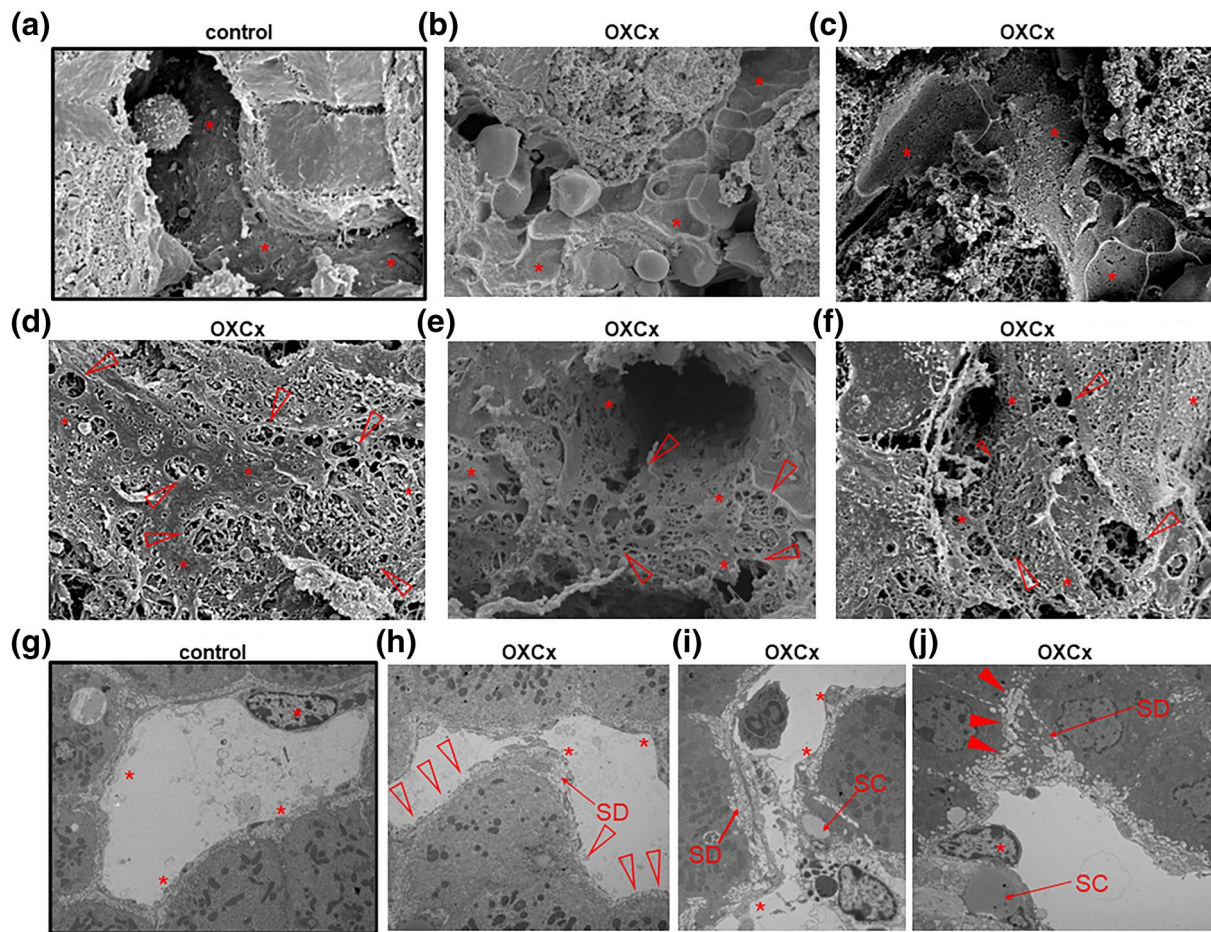


FIGURE 5 OXCx leads to morphological change of liver sinusoidal endothelial cells (LSECs), deterioration of LSEC lining, and enlargement of the space of Disse. (a–f) Representative scanning electron microscopic images of control (a) or OXCx-administrated (b–f) porcine livers (original magnification: a, $\times 3000$; b, $\times 2000$; c, 2000; d, $\times 5000$; e, $\times 5000$; f, $\times 3000$). (g–j) Representative transmission electron microscopic images of porcine livers in control (g) or OXCx-treated (h–j) groups (original magnification: g, $\times 1500$; h, $\times 1000$; i, 1500; j, $\times 1500$). *LSEC; SC, stellate cell; SD, space of Disse. Blank arrowhead indicates enlarged fenestra of LSEC or discontinuous LSEC lining. Filled arrowhead indicates collagen fiber

OXCx + rhTM group, rhTM (500 $\mu\text{g}/\text{kg}$) was injected 30 min before the beginning of each cycle. The rhTM pre-injection was associated with suppressed sinusoidal dilatation (Figure 6a), preserved LSEC architecture (Figure 6b), continuous LSEC lining (Figure 6c), and improved ICG clearance (Figure 6d) compared with the OXCx group. Using our novel pig OXCx-SOS model, here we identified the hepatoprotective influence of rhTM in OXCx-SOS.

DISCUSSION

With the recent advances in systemic chemotherapy and multidisciplinary treatment strategies, a growing number of patients with CRLM are included as candidates for radical hepatic resection after intensive preoperative chemotherapies.^{4,32} OXCx is a widely used regimen for patients with CRLM. The incidence of OXCx-SOS is reported to be as frequent as 51%–77%.^{7,8,33} OXCx-SOS is associated with impaired hepatic reserve, suppressed chemotherapy response, compromised liver regeneration after hepatectomy and higher

morbidity after hepatic resection.^{5–7,34,35} However, without an appropriate animal experimental model, little is known about its pathophysiology and preventive strategies remain to be determined. In this study, we established a reproducible animal model of OXCx-SOS using the micro-minipig, an animal that closely resembles human in terms of anatomy, physiology, and genetics.³⁶ In addition, we compared human OXCx-SOS, rat MCT-SOS, and pig OXCx-SOS and highlighted the dissimilarities and shared physiologies in the disease progressions (Table 2).

Rat MCT-SOS is the most widely used and intensively studied SOS model. This model develops hepatomegaly, ascites, hyperbilirubinemia, and marked elevation of serum AST/ALT levels, therefore mimicking human SCT-SOS. In the pathogenesis of MCT-SOS, MCT pyrrole, an active metabolite of MCT, acts on LSECs to cause deformation and cell detachment from the sinusoidal wall. MCT pyrrole also upregulates the enzymatic activity of MMP-9, which breaks down the extracellular matrix in the space of Disse to facilitate the uplift of LSECs.^{10,26} Peel-off of LSEC along with red blood cells penetrating under the LSEC barrier narrows the

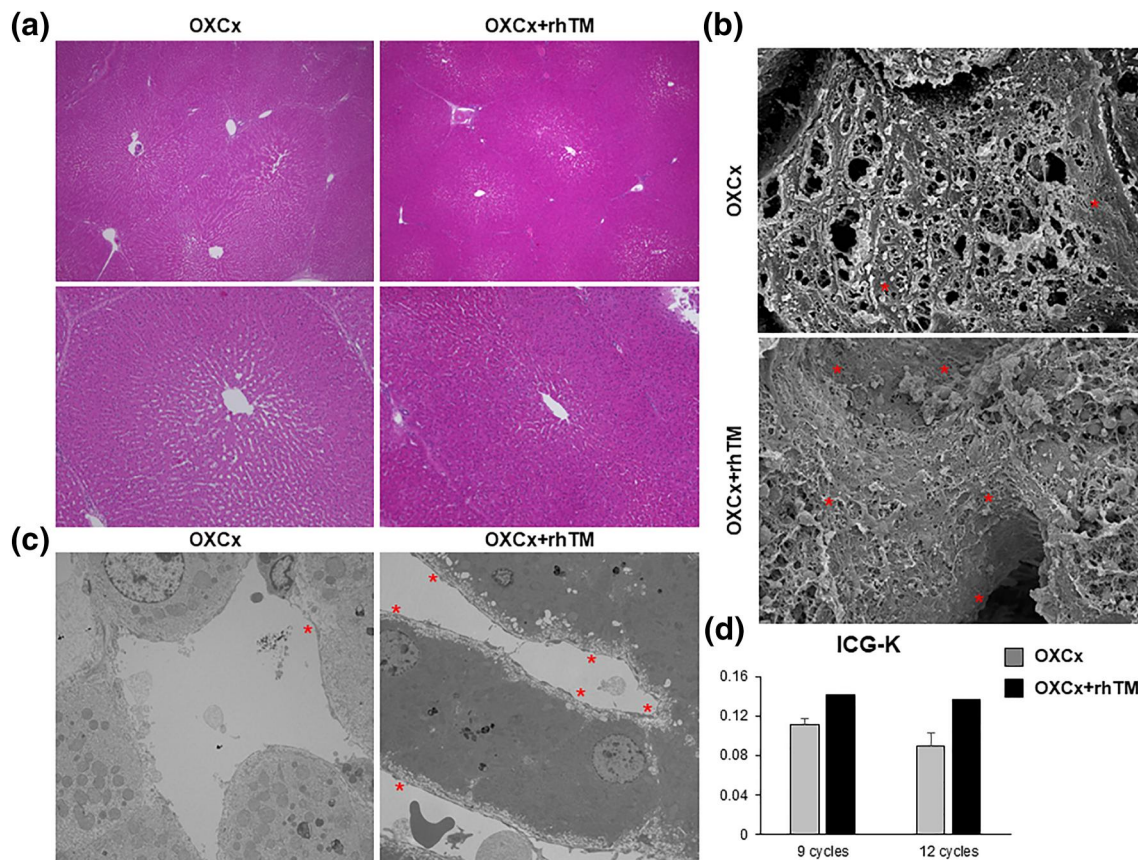


FIGURE 6 Recombinant human soluble thrombomodulin (rhTM) alleviates endothelial injury and hepatic dysfunction in OXCx-treated pigs. Twelve cycles of OXCx were infused to micro mini-pigs with or without rhTM pretreatment (500 μ g/kg, intravenous) 30 min before the beginning of folinic acid/oxaliplatin infusion in each cycle. (a) Representative hematoxylin and eosin images of livers from OXCx and OXCx + rhTM groups (upper panels, $\times 40$; lower panels, $\times 100$). (b) Representative scanning electron microscopic images of OXCx and OXCx + rhTM groups (original magnification, OXCx, $\times 5000$; OXCx + rhTM, $\times 5000$). (c) Representative transmission electron microscopic images (original magnification, OXCx, $\times 1500$; OXCx + rhTM, $\times 1000$). *LSEC. (d) Indocyanine green elimination rate (ICG-K) values in OXCx and OXCx + rhTM groups. LSEC, liver sinusoidal endothelial cell

sinusoidal lumen, leading to extensive congestion, disturbance of blood supply, hepatocellular necrosis, and elevated hepatic transaminase levels (Figure 2). We examined clinical OXCx-treated non-tumorous liver tissue and swine OXCx-SOS and found that sinusoidal dilatation, enlargement of the space of Disse, and fibrosis are shared in both MCT-SOS and OXCx-SOS. In addition, rounding-up of LSECs, MMP-9 upregulation, and loss of LSEC integrity appear to be the common mechanisms of pathogenesis in SOS (Table 2). In contrast to MCT-SOS, human/pig OXCx-SOS develops slowly without hepatomegaly, ascites, and hyperbilirubinemia, even though OXCx induces morphological alteration and injury of LSECs (Figures 1e,g, 4g and 5). In the human OXCx group, serum AST/ALT levels tended to be slightly higher compared with levels in the control group or the OXCx group before FOLFOX treatment; however, the increased levels were almost within the normal range and the differences did not reach statistical significance (Table 1). OXCx failed to increase serum AST/ALT levels in pigs (Figure 4e), whereas histological evaluation showed that congestion and hepatocellular necrosis were minimal in human and pig OXCx-SOS (Figures 1c and 4b). Those findings indicate that narrowing of

sinusoidal lumen and inhibited blood supply may be limited or compensated as damage and loss of LSECs develops slowly over time in pig and human OXCx-SOS. Regardless of the rapidity of hepatic damage, it should be emphasized that LSEC injury is highly likely to be the key trigger of SOS development not only in SCT/MCT-SOS but also in human/pig OXCx-SOS, as the morphological alteration and the loss of LSEC appear to be the common pathological changes in overall SOS (Table 2). Despite no splenomegaly was found in our limited clinical cases with OXCx ($n = 22$) as well as in the OXCx-challenged micro-minipigs, others reported that splenomegaly or hypersplenism might be one of the putative surrogate markers to predict clinical OXCx-SOS.³⁷⁻³⁹ Those studies also support the notion that LSEC injury and subsequent perisinusoidal fibrosis appear to be the key pathophysiology, which leads portal hypertension and splenomegaly.

We identified distinct disparities in the pathophysiology between SCT-SOS and OXCx-SOS (Table 2). Therefore, the findings obtained from rat MCT-SOS are not necessarily applicable to OXCx-SOS. We, along with other groups, reported the efficacy of rhTM, a drug comprising the extracellular domain of TM, to reduce SOS severity in

rat MCT-SOS.^{18,19} The lectin-like domain of rhTM exerts an anti-inflammatory influence by binding to and inactivating high mobility group box 1 (HMGB1). A suppressed HMGB1-neutrophil interaction was reported to be a key underlying mechanism protecting LSECs in MCT-SOS. In the present study, pre-injection of rhTM in the porcine OXCx-SOS model protected LSECs and preserved liver function (Figure 6). Our findings support rhTM and strategies to inhibit HMGB1 as prophylactic strategies of OXCx-SOS. MMP-9 serves as a key molecule for inducing SCT-SOS.²⁷ Our results demonstrated the upregulation of MMP-9 in OXCx-SOS in pig and human. As MMP inhibition successfully attenuated SOS in MCT-SOS,²⁷ validations of MMP inhibitor in the porcine OXCx-SOS model are warranted.

Unlike previous studies, we were unable to induce hepatic histopathological changes such as LSEC injury or hepatocellular death by administering FOLFOX to mice in the same manner as reported.^{12,13} Our results are consistent with other reports.^{15,16} The dosage of FOLFOX used in this murine model is sufficient compared with the dose in human and is close to lethal, as 58% of mice in our study (Supporting Information S1: Figure S1) and 10% of mice in the previous report¹² died during the experimental course. The lack of success to generate SOS might be from species-specific differences in genetics or metabolism. Following the human mFOLFOX6 method, by placing and using a central venous access port, we established the clinically relevant porcine OXCx-SOS model. We used a 50% dosage of the human mFOLFOX6 regimen, and human OXCx-SOS features appeared after 9–12 cycles (equivalent to 4.5–6 cycles of human mFOLFOX6), with significantly decreased ICG-K values after 12 cycles (Figure 4c). The chemotherapeutic doses of our porcine OXCx-SOS model are consistent with clinical studies showing the increased incidence of SOS after five to six cycles of FOLFOX.^{40,41} As is the case with human mFOLFOX6 therapy, OXCx-treated pigs require careful monitoring and appropriate supportive care to alleviate symptoms from adverse effects, whenever necessary, as part of routine experimental animal care. We have experienced frequent animal death during experiments when using 100%/75% dosage of the human mFOLFOX6 regimen (Supporting Information S1: Table S1), probably because it had been difficult to provide them with really required supportive care in a timely fashion. Considering the lack of self-complaint of chemotherapeutic side effects and the difficulty in continuous intensive monitoring in pigs, more simple and efficacious means of supportive care are desired for modifying the pig OXCx model to use the higher dose of FOLFOX.

In the current clinical experiment, 12 of 22 (55%) cases were diagnosed as SOS by pathological examination of resected non-tumorous tissue, with sinusoidal dilatation being the predominant histological abnormality, while coagulative necrosis and central venous injury appeared to be minimal (Table 2). After the histological evaluations of clinical liver tissue, we confirmed that livers from OXCx-treated pigs in our study exhibited consistent histological changes with human OXCx-SOS, based on the light- and electron microscopy examinations (Figures 4 and 5). Although sinusoidal dilatation, coagulative necrosis and central venous injury are well-established factors to evaluate then SCT/MCT-SOS histologically,¹⁰ with our study highlighting the definite histological differences

between SCT/MCT-SOS and OXCx-SOS, it is desired to establish the indicators of pathological evaluation specifically for OXCx-SOS. In this study, none of the OXCx-treated patients showed hepatomegaly, ascites, and hyperbilirubinemia, factors included in the modified Seattle criteria, which is used to diagnose SOS. In addition, none of them had jaundice, elevation of liver enzyme levels, weight gain, and increase in creatinine levels, as described in the severity criteria for SOS.⁴² Thus, establishment of the clinical diagnosis and severity grading specifically for OXCx-SOS is warranted.

In our clinical cohort, patients with CRLM with synchronous and multiple liver lesions were more frequent in the OXCx group compared with the control group. As shown in Supporting Information S1: Figure S3, patients in the OXCx group tended to have worse recurrence-free survival ($p = 0.3327$) and OS ($p = 0.4454$), although without significance. Impaired post-hepatectomy outcomes likely reflect the high acuity of liver lesions in our cohort. Meanwhile, patients with CRLM with sinusoidal dilatation have a significantly shorter recurrence free survival and OS⁸ compared with the control group and our recent study demonstrated that induction of MCT-SOS increased the number of liver tumors in the splenic RCN-H4 injection model compared with control rats.⁴² Therefore, prophylaxis of OXCx-SOS is important not only to reduce surgical morbidity but also to improve oncological outcome.

In conclusion, we have established a reproducible model of FOLFOX-induced SOS in micro-minipigs and highlighted the disparities and common features between MCT-SOS and OXCx-SOS. Our pig OXCx-SOS model serves as a preclinical platform to dissect the pathophysiology of OXCx-SOS, identify biomarkers, validate findings acquired from the rat MCT-SOS model, and seek preventive strategies against OXCx-SOS.

ACKNOWLEDGMENTS

We are grateful to Yakult Honsha (Tokyo, Japan) for the kind gift of L-OHP, and Asahi Kasei Pharma (Tokyo, Japan) for the kind gift of rhTM. We also acknowledge the support of the Center for Anatomical, Pathological, and Forensic Medical Research, Kyoto University Graduate School of Medicine, for preparing the microscope slides and use of their electron microscopes. We thank Gabrielle White Wolf, PhD, from Edanz for editing a draft of this manuscript. This work was supported by JSPS KAKENHI 18K08645 (to Satoru Seo), 19K24012 (to Kojiro Nakamura) and 16H05414 (to Etsuro Hatano).

CONFLICT OF INTEREST

The authors have no conflict of interest.

DATA AVAILABILITY STATEMENT

The datasets used and/or analyzed during the current study are available from the corresponding author on reasonable request.

ETHICS STATEMENT

All human studies were approved by the Ethics Committee of Kyoto University Graduate School and Faculty of Medicine (approval code: R3004) and written informed consent was received from participants

before inclusion in the study. All animal experiments were approved by the Animal Research Committee of Kyoto University (Med Kyo 18187). All animal experiments were performed according to the approved protocols and in compliance with the ARRIVE guidelines. All methods were carried out in accordance with relevant guidelines and regulations.

ORCID

Rei Toda  <https://orcid.org/0000-0003-3532-8930>

Naohiko Nakamura  <https://orcid.org/0000-0002-5542-0163>

REFERENCES

- Scheele J, Stangl R, Altendorf-Hofmann A. Hepatic metastases from colorectal carcinoma: impact of surgical resection on the natural history. *Br J Surg*. 1990;77(11):1241–6. <https://doi.org/10.1002/bjs.1800771115>
- Okuno M, Hatano E, Toda R, Nishino H, Nakamura K, Ishii T, et al. Conversion to complete resection with mFOLFOX6 with bevacizumab or cetuximab based on K-RAS status for unresectable colorectal liver metastasis (BECK study): long-term results of survival. *J Hepato-Biliary-Pancreatic Sci*. 2020;27(8):496–509. <https://doi.org/10.1002/jhbp.747>
- Adam R, Delvart V, Pascal G, Valeanu A, Castaing D, Azoulay D, et al. Rescue surgery for unresectable colorectal liver metastases downstaged by chemotherapy: a model to predict long-term survival. *Ann Surg*. 2004;240(4):644–57. <https://doi.org/10.1097/01.sla.0000141198.92114.f6>
- Hatano E, Okuno M, Nakamura K, Ishii T, Seo S, Taura K, et al. Conversion to complete resection with mFOLFOX6 with bevacizumab or cetuximab based on K-ras status for unresectable colorectal liver metastasis (BECK study). *J Hepato-Biliary-Pancreatic Sci*. 2015;22(8):634–45. <https://doi.org/10.1002/jhbp.254>
- Rubbia-Brandt L, Audard V, Sartoretti P, Roth AD, Brezault C, Le Charpentier M, et al. Severe hepatic sinusoidal obstruction associated with oxaliplatin-based chemotherapy in patients with metastatic colorectal cancer. *Ann Oncol*. 2004;15(3):460–6. <https://doi.org/10.1093/annonc/mdh095>
- Nakano H, Oussoultzoglou E, Rosso E, Casnedi S, Chenard-Neu MP, Dufour P, et al. Sinusoidal injury increases morbidity after major hepatectomy in patients with colorectal liver metastases receiving preoperative chemotherapy. *Ann Surg*. 2008;247(1):118–24. <https://doi.org/10.1097/sla.0b013e31815774de>
- Soubrane O, Brouquet A, Zalinski S, Terris B, Brézault C, Mallet V, et al. Predicting high grade lesions of sinusoidal obstruction syndrome related to oxaliplatin-based chemotherapy for colorectal liver metastases: correlation with post-hepatectomy outcome. *Ann Surg*. 2010;251(3):454–60. <https://doi.org/10.1097/sla.0b013e3181c79403>
- Tamandl D, Klinger M, Eipeldauer S, Herberger B, Kaczirek K, Gruenberger B, et al. Sinusoidal obstruction syndrome impairs long-term outcome of colorectal liver metastases treated with resection after neoadjuvant chemotherapy. *Ann Surg Oncol*. 2011;18(2):421–30. <https://doi.org/10.1245/s10434-010-1317-4>
- Dignan FL, Wynn RF, Hadzic N, Karani J, Quaglia A, Pagliuca A, et al. BCSH/BSBMT guideline: diagnosis and management of veno-occlusive disease (sinusoidal obstruction syndrome) following haematopoietic stem cell transplantation. *Br J Haematol*. 2013;163(4):444–57. <https://doi.org/10.1111/bjh.12558>
- DeLeve LD, McCuskey RS, Wang X, Hu L, McCuskey MK, Epstein RB, et al. Characterization of a reproducible rat model of hepatic veno-occlusive disease. *Hepatology*. 1999;29(6):1779–91. <https://doi.org/10.1002/hep.510290615>
- Narita M, Hatano E, Ikai I, Miyagawa-Hayashino A, Yanagida A, Nagata H, et al. A phosphodiesterase III inhibitor protects rat liver from sinusoidal obstruction syndrome through heme oxygenase-1 induction. *Ann Surg*. 2009;249(5):806–13. <https://doi.org/10.1097/sla.0b013e3181a38ed5>
- Robinson SM, Mann J, Vasilaki A, Mathers J, Burt AD, Oakley F, et al. Pathogenesis of FOLFOX induced sinusoidal obstruction syndrome in a murine chemotherapy model. *J Hepatol*. 2013;59(2):318–26. <https://doi.org/10.1016/j.jhep.2013.04.014>
- Robinson SM, Mann DA, Manas DM, Oakley F, Mann J, White SA. The potential contribution of tumour-related factors to the development of FOLFOX-induced sinusoidal obstruction syndrome. *Br J Cancer*. 2013;109(9):2396–403. <https://doi.org/10.1038/bjc.2013.604>
- Park SH, Lee SS, Sung JY, Na K, Kim HJ, Kim SY, et al. Noninvasive assessment of hepatic sinusoidal obstructive syndrome using acoustic radiation force impulse elastography imaging: a proof-of-concept study in rat models. *Eur Radiol*. 2018;28(5):2096–106. <https://doi.org/10.1007/s00330-017-5179-z>
- Hubert C, Dahrenmoller C, Marique L, Jabbour N, Gianello P, Leclercq I. Hepatic regeneration in a rat model is impaired by chemotherapy agents used in metastatic colorectal cancer. *Eur J Surg Oncol*. 2015;41(11):1471–8. <https://doi.org/10.1016/j.ejso.2015.08.152>
- Lentschener C, Nicco C, Terris B, Samama CM, Coriat R. Comment on 'The potential contribution of tumour-related factors to the development of FOLFOX-induced sinusoidal obstruction syndrome'. *Br J Cancer*. 2016;115(8):e7. <https://doi.org/10.1038/bjc.2016.242>
- Robinson SM, Mann DA, Manas DM, Oakley F, Mann J, White SA. Response to 'Comment on 'The potential contribution of tumour-related factors to the development of FOLFOX-induced sinusoidal obstruction syndrome''. *Br J Cancer*. 2016;115(8):e8. <https://doi.org/10.1038/bjc.2016.268>
- Nakamura K, Hatano E, Miyagawa-Hayashino A, Okuno M, Koyama Y, Narita M, et al. Soluble thrombomodulin attenuates sinusoidal obstruction syndrome in rat through suppression of high mobility group box 1. *Liver Int*. 2014;34(10):1473–87. <https://doi.org/10.1111/liv.12420>
- Takada S, Miyashita T, Yamamoto Y, Kanou S, Muniesue S, Ohbatake Y, et al. Soluble thrombomodulin attenuates endothelial cell damage in hepatic sinusoidal obstruction syndrome. *In Vivo*. 2018;32(6):1409–17. <https://doi.org/10.21873/invivo.11393>
- Guglielmelli T, Bringham S, Palumbo A. Update on the use of defibrotide. *Expert Opin Biol Ther*. 2012;12(3):353–61. <https://doi.org/10.1517/14712598.2012.657623>
- Richardson PG, Riches ML, Kernan NA, Brochstein JA, Mineishi S, Termuhlen AM, et al. Phase 3 trial of defibrotide for the treatment of severe veno-occlusive disease and multi-organ failure. *Blood*. 2016;127(13):1656–65. <https://doi.org/10.1182/blood-2015-10-676924>
- Corbacioglu S, Carreras E, Mohty M, Pagliuca A, Boelens JJ, Damaj G, et al. Defibrotide for the treatment of hepatic veno-occlusive disease: final results from the international compassionate-use program. *Biol Blood Marrow Transplant*. 2016;22(10):1874–82. <https://doi.org/10.1016/j.bbmt.2016.07.001>
- Dindo D, Demartines N, Clavien PA. Classification of surgical complications: a new proposal with evaluation in a cohort of 6336 patients and results of a survey. *Ann Surg*. 2004;240(2):205–13. <https://doi.org/10.1097/01.sla.0000133083.54934.ae>
- Rahbari NN, Garden OJ, Padbury R, Brooke-Smith M, Crawford M, Adam R, et al. Posthepatectomy liver failure: a definition and grading by the international study group of liver surgery (ISGLS). *Surgery*. 2011;149(5):713–24. <https://doi.org/10.1016/j.surg.2010.10.001>
- Kucybała I, Ciuk S, Tęczar J. Spleen enlargement assessment using computed tomography: which coefficient correlates the strongest with the real volume of the spleen? *Abdom Radiol*. 2018;43(9):2455–61. <https://doi.org/10.1007/s00261-018-1500-9>

26. Nakamura K, Hatano E, Narita M, Miyagawa-Hayashino A, Koyama Y, Nagata H, et al. Sorafenib attenuates monocrotaline-induced sinusoidal obstruction syndrome in rats through suppression of JNK and MMP-9. *J Hepatol*. 2012;57(5):1037–43. <https://doi.org/10.1016/j.jhep.2012.07.004>
27. Deleve LD, Wang X, Tsai J, Kanel G, Strasberg S, Tokes ZA. Sinusoidal obstruction syndrome (veno-occlusive disease) in the rat is prevented by matrix metalloproteinase inhibition. *Gastroenterology*. 2003;125(3):882–90. [https://doi.org/10.1016/s0016-5085\(03\)01056-4](https://doi.org/10.1016/s0016-5085(03)01056-4)
28. Okuno M, Hatano E, Nakamura K, Miyagawa-Hayashino A, Kasai Y, Nishio T, et al. Regorafenib suppresses sinusoidal obstruction syndrome in rats. *J Surg Res*. 2015;193(2):693–703. <https://doi.org/10.1016/j.jss.2014.08.052>
29. Narita M, Oussoultzoglou E, Chenard M-P, Fuchshuber P, Rather M, Rosso E, et al. Liver injury due to chemotherapy-induced sinusoidal obstruction syndrome is associated with sinusoidal capillarization. *Ann Surg Oncol*. 2012;19(7):2230–7. <https://doi.org/10.1245/s10434-011-2112-6>
30. U.S. Food and Drug Administration. Highlights of prescribing information: eloxatin (oxaliplatin) injection, for intravenous use. Initial U.S. Approval: 2002. 2002. https://www.accessdata.fda.gov/drugsatfda_docs/label/2020/021759s023lbl.pdf
31. Shirao K. Phase I study of single-dose oxaliplatin in Japanese patients with malignant tumors. *Jpn J Clin Oncol*. 2006;36(5):295–300. <https://doi.org/10.1093/jjco/hyl016>
32. Oki E, Emi Y, Yamanaka T, Uetake H, Muro K, Takahashi T, et al. Randomised phase II trial of mFOLFOX6 plus bevacizumab versus mFOLFOX6 plus cetuximab as first-line treatment for colorectal liver metastasis (ATOM trial). *Br J Cancer*. 2019;121(3):222–9. <https://doi.org/10.1038/s41416-019-0518-2>
33. Hubert C, Sempoux C, Humblet Y, Van Den Eynde M, Zech F, Leclercq I, et al. Sinusoidal obstruction syndrome (SOS) related to chemotherapy for colorectal liver metastases: factors predictive of severe SOS lesions and protective effect of bevacizumab. *HPB*. 2013;15(11):858–64. <https://doi.org/10.1111/hpb.12047>
34. Aloia T, Sebah M, Plasse M, Karam V, Lévi F, Giacchetti S, et al. Liver histology and surgical outcomes after preoperative chemotherapy with fluorouracil plus oxaliplatin in colorectal cancer liver metastases. *J Clin Oncol*. 2006;24(31):4983–90. <https://doi.org/10.1200/jco.2006.05.8156>
35. Pawlik TM, Olino K, Gleisner AL, Torbenson M, Schulick R, Choti MA. Preoperative chemotherapy for colorectal liver metastases: impact on hepatic histology and postoperative outcome. *J Gastrointest Surg*. 2007;11(7):860–8. <https://doi.org/10.1007/s11605-007-0149-4>
36. Verma N, Rettenmeier AW, Schmitz-Spanke S. Recent advances in the use of *Sus scrofa* (pig) as a model system for proteomic studies. *Proteomics*. 2011;11(4):776–93. <https://doi.org/10.1002/pmic.201000320>
37. Park S, Kim HY, Kim H, Park JH, Kim JH, Kim KH, et al. Changes in noninvasive liver fibrosis indices and spleen size during chemotherapy: potential markers for oxaliplatin-induced sinusoidal obstruction syndrome. *Medicine*. 2016;95(2):e2454. <https://doi.org/10.1097/md.0000000000002454>
38. El Chediak A, Haydar AA, Hakim A, Massih SA, Hilal L, Mukherji D, et al. Increase in spleen volume as a predictor of oxaliplatin toxicity. *Therapeut Clin Risk Manag*. 2018;14:653–7. <https://doi.org/10.2147/tcrm.s150968>
39. Bando H, Yamada Y, Tanabe S, Nishikawa K, Gotoh M, Sugimoto N, et al. Efficacy and safety of S-1 and oxaliplatin combination therapy in elderly patients with advanced gastric cancer. *Gastric Cancer*. 2016;19(3):919–26. <https://doi.org/10.1007/s10120-015-0549-1>
40. Karoui M, Penna C, Amin-Hashem M, Mitry E, Benoist S, Franc B, et al. Influence of preoperative chemotherapy on the risk of major hepatectomy for colorectal liver metastases. *Ann Surg*. 2006;243:1–7. <https://doi.org/10.1097/01.sla.0000193603.26265.c3>
41. Takamoto T, Hashimoto T, Sano K, Maruyama Y, Inoue K, Ogata S, et al. Recovery of liver function after the cessation of preoperative chemotherapy for colorectal liver metastasis. *Ann Surg Oncol*. 2010;17(10):2747–55. <https://doi.org/10.1245/s10434-010-1074-4>
42. Nishino H, Okuno M, Seo S, Toda R, Yoshino K, Kasai Y, et al. Sinusoidal obstruction syndrome promotes liver metastatic seeding of colorectal cancer cells in a rat model. *Anticancer Res*. 2021;41(4):1803–10. <https://doi.org/10.21873/anticancer.14946>

SUPPORTING INFORMATION

Additional supporting information can be found online in the Supporting Information section at the end of this article.

How to cite this article: Toda R, Seo S, Uemoto Y, Morino K, Nishino H, Nakamura N, et al. Clinically relevant model of oxaliplatin-induced sinusoidal obstruction syndrome. *Hepatol Res*. 2022;1–15. <https://doi.org/10.1111/hepr.13842>